

# Supporting Information

## Magnesium-isotopic Equilibrium in Chlorophylls

*Black, J. R., Yin, Q-Z., Rustad, J. R. and W. H. Casey.*

### Materials and Methods:

#### ***Sampling, Extraction and Purification:***

Mature leaves were collected, blended into a pulp and the photosynthetic pigments were extracted into methanol. The yields of Chl-a and Chl-b in the extracts were determined (sample IV07, extracts 1 and 2, Supp. Table S1) by UV-Vis spectrophotometry<sup>S1</sup>. Chl-a and Chl-b pigments were purified on anion-exchange columns<sup>S2-S3</sup> and final yields of Chl-a and Chl-b in combined samples (IV08 and IV09, Supp. Table S1), pure Chl-a samples (IV10, IV12, Supp. Table S1) and pure Chl-b samples (IV11, IV13, Supp. Table S1) were determined using UV-Vis.

#### ***Leaf Digestion:***

About 0.5 gram of leaf pulp was digested in 5 ml of concentrated and ultrapure nitric acid by refluxing for an hour at 30°C, 70-80°C and 170-180°C. Samples were diluted with 5ml concentrated and ultrapure hydrochloric acid, then to a final volume of 25ml with doubly deionized water. Aliquots of the supernatant were taken for analysis.

#### ***Magnesium Purification:***

The methods for liberating and purifying magnesium from the chlorophyll samples are described elsewhere<sup>S2</sup> with a  $102 \pm 9\%$  yield achieved (see Supp. Table S1, excluding sample IV09 which was impure). Samples for analysis were prepared in ultrapure 0.1M HCl so that the final concentration of magnesium was ~650 ppb.

#### **Isotopic Measurements:**

Measurements were conducted on a Nu MC-ICP-MS using a standard-sample bracketing technique and the two international standards, DSM3 and Cambridge 1 to monitor the established isotopic difference<sup>S4</sup>. The isotopic ratio of the DSM3 standard was extrapolated to the time of sample measurement in order to standardize the data. Details of this method are reported elsewhere<sup>S2</sup>.

#### ***DFT Calculations:***

All molecules were optimized in the gas phase using the PQS Ab Initio Program Package version 3.3<sup>S5</sup> on a 16-processor Quantum Cube with 16 GB of RAM. We used a 6-31G\* Gaussian basis set with the O3LYP exchange-correlation functional<sup>S6</sup>. The precision of the DFT grid was increased beyond the default values (FACTOR=1.5 in PQS v. 3.3). Geometry optimization was carried out with delocalized internal coordinates<sup>S7</sup> using the eigenvector-following algorithm<sup>S8</sup> and was terminated when the maximum gradient was less than 0.00003 and the energy change was less than 0.000001 Hartree on successive cycles. The Hessian matrix was evaluated analytically with default PQS version 3.3 integral thresholds.

We made use of a particularly accurate method of vibrational frequency scaling known as mSQM.<sup>S9</sup> In this approach, force constants associated with individual valence coordinates (stretches, bends, and torsions) are scaled to reproduce experimental values for a series of small organic molecules.

This approach allows calculation of vibrational frequencies to  $\sim 8\text{ cm}^{-1}$ . The efficacy of this general approach in porphyrin systems has been established in a series of papers by Pulay and co-workers.<sup>S10-S11</sup>

For comparison with Chl-a and Chl-b, we chose magnesium complexes representative of aqueous magnesium species and organic magnesium complexes. Supplementary Figure S2 shows a predominance diagram for aqueous magnesium species in a nutrient solution<sup>S2</sup> as a function of pH. Plants have robust mechanisms for regulated the pH of the cytoplasm in their cells at around 7 to 7.5<sup>S12</sup>. Supplementary Figure S2 shows that the hexa-aqua magnesium complex is the main form of Mg in solution (69.9%) at this pH (7.1), however, low levels of Mg-citrate (12%), Mg-biphosphate (7.2%), Mg-sulphate (6.8%), Mg-chloride (2.4%) and Mg-bicarbonate (1.7%) also exist in solution. These species were all considered as sources of the Mg for chlorophyll. The composition of the cytoplasm in a plant's cells will have much higher concentrations of magnesium species and could potentially also include organic ligands, making it hard to unequivocally determine the internal speciation of magnesium. Nevertheless, we consider these aqueous forms of magnesium to be a good initial estimate for comparing fractionation factors. Since the hexa  $\text{Mg}(\text{H}_2\text{O})_6^{2+}(\text{aq})$  complex is the predominant form under physiological conditions, DFT calculations were performed on a number of structures of  $\text{Mg}(\text{H}_2\text{O})_6^{2+}(\text{aq})$  (A-C, Supp. Fig. S3). The magnesium citrate complex was also chosen as another potential bioavailable form (D, Supp. Fig. S3). The choice of biomolecules was made based upon the biosynthetic pathways that produce Chl-a and Chl-b and calculations were performed on Mg-Protoporphyrin IX (A, Supp. Fig. S4), Chlorophyllide-a (B, Supp. Fig. S4), Chlorophyll-a (C, Supp. Fig. S4), Chlorophyll-b, Chl-a bound to a residue of histidine (D, Supp. Fig. S4) and Chl-b bound to a residue of histidine.

## Supplementary References:

- (S1) Porra, R. J.; Thompson, W. A.; Kriedemann, P. E. *Biochim. Biophys. Acta* **1989**, 975, 384-394.
- (S2) Black, J. R.; Yin, Q.-Z.; Casey, W. H. *Geochim. Cosmo. Acta* **2006**, 70, 4072-4079.
- (S3) Omata, T.; Murata, N. *Photochem. & Photobio.* **1980**, 31, 183-185.
- (S4) Galy, A.; Yoffe O.; Janney P. E.; Williams R. W.; Cloquet C.; Alard O.; Halicz L.; Wadhwa M.; Hutcheon I. D.; Ramon E.; Carignan J. *J. Anal. Atom. Spec.* **2003**, 18, 1352-1356.
- (S5) Parallel Quantum Solutions, Fayetteville, Arkansas, <http://www.pqs.com> 2007.
- (S6) Handy, N. C.; Cohen, A. J. *Molecular Physics* **2001**, 99, 403-412.
- (S7) Baker, J.; Kessi, A; Delley, B. *J. Chem. Phys.* **1996**, 105, 192-211.
- (S8) Baker, J. *J. Comp. Chem.* **1986**, 7, 385-395.
- (S9) Baker, J.; Jarzecki, A.A.; Pulay, P. *J. Phys. Chem. A.* **1998**, 102, 1412-1424.
- (S10) Kozlowski, P. M.; Zgierski, M.Z.; Pulay, P. *Chem. Phys. Lett.* **1995**, 247, 379-385.
- (S11) Jarzecki, A.A.; Kozlowski, P. M.; Pulay, P.; Ye, B. H.; Li, X. Y. *Spectrochim. Acta A.* **1997**, 53, 1195-1209.
- (S12) Felle, H. H. *Annals of Botany* **2005**, 96, 519-532.

**Supplementary Table S1: Magnesium-isotopic composition of samples**

Sample	$\delta^{26}\text{Mg}^a$ (‰) $\pm 2\sigma$	$\delta^{25}\text{Mg}^a$ (‰) $\pm 2\sigma$	$\Delta^{26}\text{Mg}^b$ (‰) $\pm 2\sigma$	$\Delta^{25}\text{Mg}^b$ (‰) $\pm 2\sigma$	N (R) <sup>c</sup>
DSM3	0 $\pm$ 0.029	0 $\pm$ 0.028			28 (1)
Cambridge 1	-2.575 $\pm$ 0.100	-1.337 $\pm$ 0.056			9 (1)
Cambridge 1 <sup>10</sup>	-2.60 $\pm$ 0.14	-1.34 $\pm$ 0.07			35 (1)
Leaf Digestion:					
IV14	-0.610 $\pm$ 0.140	-0.326 $\pm$ 0.083			4 (2)
IV16	-0.644 $\pm$ 0.048	-0.343 $\pm$ 0.053			3 (1)
IV16	-0.510 $\pm$ 0.027	-0.272 $\pm$ 0.023			1 (1)
Combined Chl-a + Chl-b:					
IV08 extract 1	-0.182 $\pm$ 0.145	-0.099 $\pm$ 0.082	0.428 $\pm$ 0.201	0.227 $\pm$ 0.117	4 (1)
Calc. <sup>d</sup> extract 1	-0.121	-0.081			-
Calc. <sup>d</sup> extract 2	-0.091	-0.071			-
Pure Chl-a:					
IV10 extract 1	-0.022 $\pm$ 0.119	-0.027 $\pm$ 0.095	0.589 $\pm$ 0.184	0.298 $\pm$ 0.126	4 (1)
IV12 extract 2	0.014 $\pm$ 0.029	-0.012 $\pm$ 0.022	0.625 $\pm$ 0.143	0.314 $\pm$ 0.086	1 (1)
Pure Chl-b:					
IV11 extract 1	-0.455 $\pm$ 0.090	-0.262 $\pm$ 0.074	0.156 $\pm$ 0.166	0.063 $\pm$ 0.111	4 (1)
IV13 extract 2	-0.380 $\pm$ 0.029	-0.232 $\pm$ 0.026	0.231 $\pm$ 0.143	0.094 $\pm$ 0.087	1 (1)
Spinach Chlorophyll-a <sup>4</sup>	-1.451 $\pm$ 0.098	-0.741 $\pm$ 0.062			-
Spinach Chlorophyll-b <sup>4</sup>	-2.352 $\pm$ 0.067	-1.204 $\pm$ 0.026			-

<sup>a</sup> The magnesium isotopic composition of the samples is expressed as a per-mil deviation from the DSM3 standard using the formula:  $\delta^x\text{Mg} = \{(^x\text{Mg}/^{24}\text{Mg})_{\text{Sample}} / (^x\text{Mg}/^{24}\text{Mg})_{\text{DSM3}} - 1\}$ ; <sup>b</sup>  $\Delta^x\text{Mg} = \delta^x\text{Mg}_{\text{sample}} - \delta^x\text{Mg}_{\text{leaf digestion}}$ ; <sup>c</sup> N = number of replicates; R = number of separate samples; <sup>d</sup> Calculated values given the measured isotopic ratios of purified Chl-a and Chl-b and the % yield of Chl-a and Chl-b in the corresponding extracts (Supp. Table S2); The uncertainty is reported at 95% confidence level ( $2\sigma$ ).

**Supplementary Table S2: The initial amounts and final yields of Chl-a and Chl-b and magnesium in samples of English Ivy leaves after extraction of the pigment and purification.**

Sample	Absorbance <sup>a</sup>	Chl-a <sup>b</sup> (mg)	Yield of Chl-a <sup>c</sup>	Chl-b <sup>b</sup> (mg)	Yield of Chl-b <sup>c</sup>	Mg-yield
Pigment extract:						
IV07 extract 1	1.184 (105 ml)	1.44	100%	0.43	100%	-
IV07 extract 2	2.119 (108 ml)	2.64	100%	0.81	100%	-
Purified:						
Chl-a + Chl-b:						
IV08 extract 1	2.894 (20 ml)	0.67	51.7%	0.20	54.1%	104% <sup>d</sup>
IV09 extract 2	1.414 (20 ml)	0.32	18.1%	0.12	18.6%	311% <sup>d</sup>
Chl-a:						
IV10 extract 1	1.880 (20 ml)	0.463 $\pm$ 0.015	36.0%			99% <sup>d</sup>
IV12 extract 2	3.186 (20 ml)	0.484 $\pm$ 0.011	33.7%			100% <sup>d</sup>
Chl-b:						
IV11 extract 1	0.150 (20 ml)			0.121 $\pm$ 0.024	27.5%	98% <sup>d</sup>
IV13 extract 2	0.164 (20 ml)			0.126 $\pm$ 0.039	20.2%	109% <sup>d</sup>
Ivy Leaf Digests:						
IV14	N/A	N/A	N/A	N/A	N/A	0.52 mg/g <sup>e</sup>
IV16	N/A	N/A	N/A	N/A	N/A	0.51 mg/g <sup>e</sup>

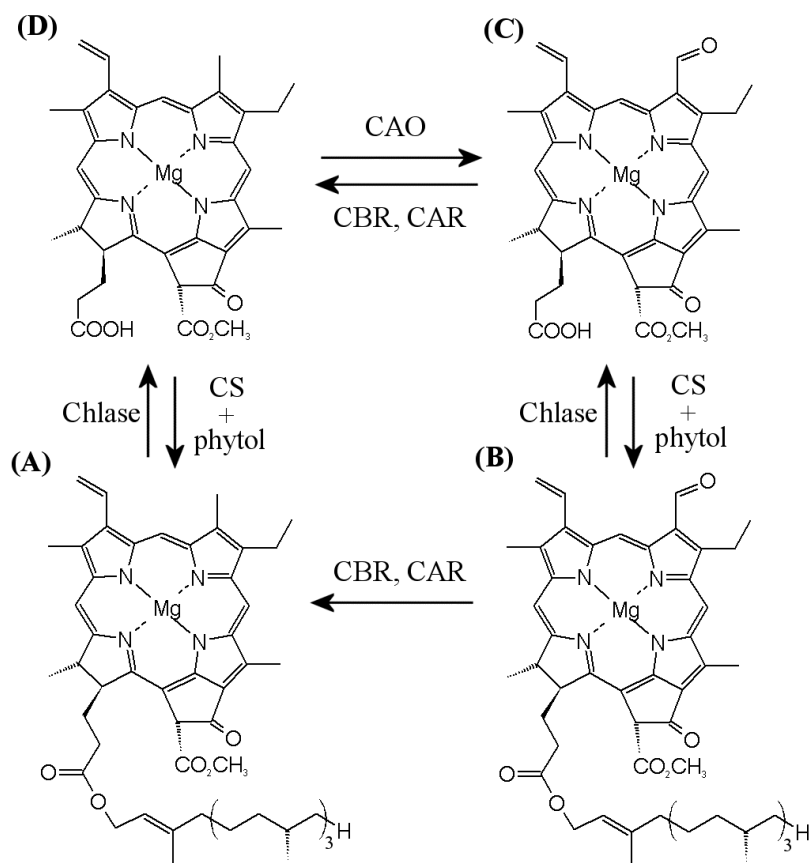
<sup>a</sup> at 665.5nm (total volume of methanol extract); <sup>b</sup> pigment extract in methanol  $\pm 2\sigma$ ; <sup>c</sup> percentage yield of chlorophyll-a or -b in methanol relative to initial IV07 extract; <sup>d</sup> expressed as chlorophyll-bound Mg; <sup>e</sup> expressed as milligrams of magnesium per gram of leaf digested.

**Supplementary Table S3:** Calculated vibrational frequencies and reduced partition ratios of magnesium complexes using DFT.

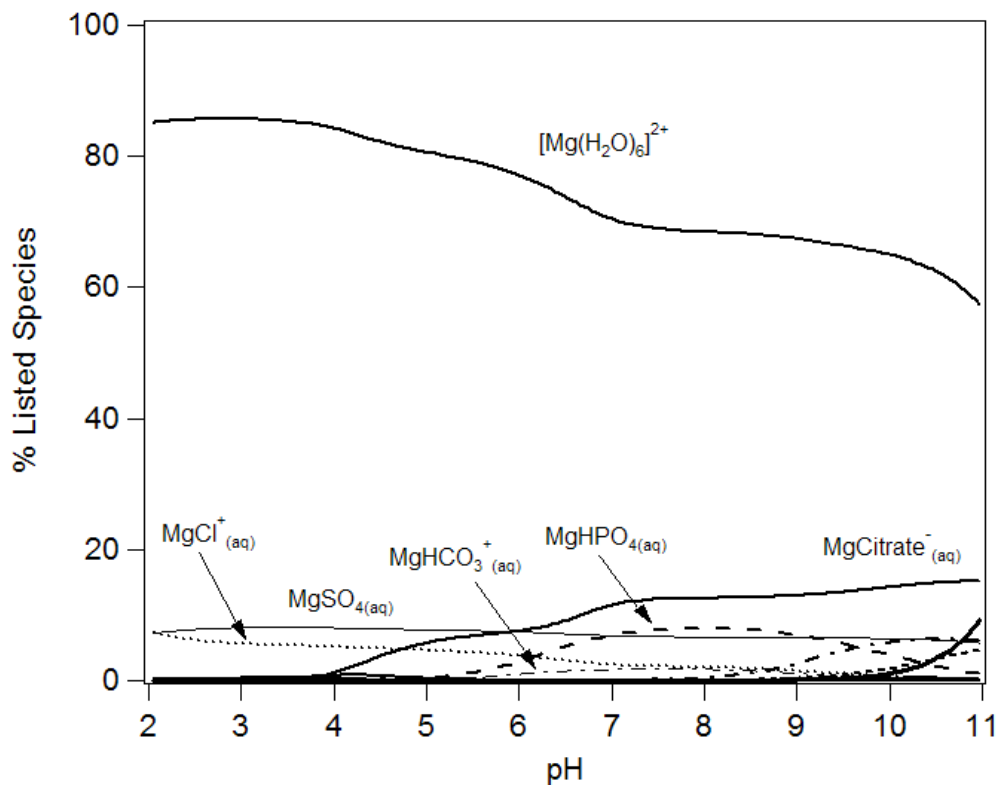
Species:	$\beta^{26/24}$	$\beta^{25/24}$
Mg(H <sub>2</sub> O) <sub>6</sub> T symm + 12H <sub>2</sub> O <sup>a</sup>	1.02554098	1.01326290
Mg(H <sub>2</sub> O) <sub>6</sub> flat + 12 H <sub>2</sub> O <sup>a</sup>	1.02654429	1.01372047
Mg(H <sub>2</sub> O) <sub>6</sub> + 26H <sub>2</sub> O <sup>a</sup>	1.02405438	1.01244909
MgCitrate + 14H <sub>2</sub> O <sup>a</sup>	1.02659290	1.01373410
Mg-Protoporphyrin IX	1.02908817	1.01500610
Chlorophyllide-a	1.02975733	1.01534742
Chlorophyllide-b	1.02906882	1.01499584
Chlorophyllide-a - HIS <sup>b</sup>	1.02805272	1.01447787
Chlorophyllide-b - HIS <sup>b</sup>	1.02799000	1.01444519
Chlorophyll-a	1.02970532	1.01532131
Chlorophyll-b	1.02905431	1.01498723
Chlorophyll-a - HIS <sup>b</sup>	1.02809242	1.01449736
Chlorophyll-b - HIS <sup>b</sup>	1.02798240	1.01444264

<sup>a</sup> outer solvation sphere waters; <sup>b</sup> HIS residue bound to Mg

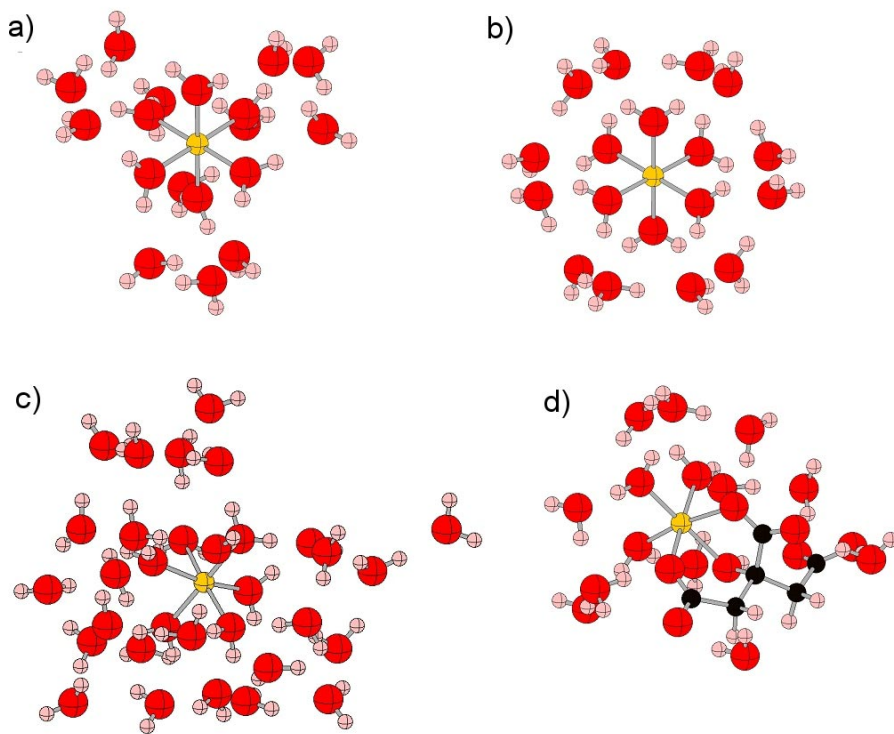
**Supplementary Figure S1:** The chlorophyll cycle adapted from Rüdiger, W. *Photosynthesis Research* **74**, 187 (2002): showing the biosynthetic pathways and chemical structure of (A) chlorophyll-a; (B) chlorophyll-b; (C) chlorophyllide-b; (D) chlorophyllide-a; CAO = chlorophyllide-a oxygenase; CS = chlorophyll syntase; Chlase = chlorophyllase; CBR = chlorophyllide b reductase; CAR = hydroxyl-chlorophyllide a reductase.



**Supplementary Figure S2:** Predominance diagram for aqueous magnesium species in a culture medium for growing cyanobacteria vs. pH. The (aq) subscript denotes that the aqueous complex also has bound waters. Temperature = 25°C. Diagram created using properties in Visual MINTEQ ver. 2.50 for aqueous magnesium species.



**Supplementary Figure S3:** Ball-and-stick diagrams of (A)  $\text{Mg}(\text{H}_2\text{O})_6$  T symm. +  $12\text{H}_2\text{O}$ ; (B)  $\text{Mg}(\text{H}_2\text{O})_6$  flat +  $12\text{H}_2\text{O}$ ; (C)  $\text{Mg}(\text{H}_2\text{O})_6^{2+}$  +  $26\text{H}_2\text{O}$ ; (D) Magnesium-citrate complex +  $14\text{H}_2\text{O}$ .



**Supplementary Figure S4:** Ball-and-stick diagrams of (A) Mg-Protoporphyrin IX; (B) Chlorophyllide-a; (C) Chlorophyll-a; (D) Chlorophyll-a with penta-coordinated Mg also bound to HIS.

